HHS Public Access

Author manuscript

*Cell Rep*. Author manuscript; available in PMC 2016 March 09.

Published in final edited form as:

*Cell Rep*. 2016 March 1; 14(8): 1901–1915. doi:10.1016/j.celrep.2016.01.067.

# Hox Proteins Coordinate Motor Neuron Differentiation and Connectivity Programs Through *Ret/Gfrα* Genes

**Catarina Catela**[1], **Maggie M. Shin**[1], **David H. Lee**[1], **Jeh-Ping Liu**[2], and **Jeremy S. Dasen**[1]

[1]Neuroscience Institute, Department of Neuroscience and Physiology, NYU School of Medicine, New York, NY 10016, USA

[2]Department of Neuroscience, University of Virginia School of Medicine, Charlottesville, VA 22908, USA

## Summary

The accuracy of neural circuit assembly relies on the precise spatial and temporal control of synaptic specificity determinants during development. Hox transcription factors govern key aspects of motor neuron (MN) differentiation; however, the terminal effectors of their actions are largely unknown. We show that Hox/Hox cofactor interactions coordinate MN subtype diversification and connectivity through *Ret/Gfrα* receptor genes. Hox and Meis proteins determine the levels of *Ret* in MNs and define the intrasegmental profiles of *Gfrα1* and *Gfrα3* expression. Loss of *Ret* or *Gfrα3* leads to MN specification and innervation defects similar to those observed in *Hox* mutants, while expression of *Ret* and *Gfrα1* can bypass the requirement for *Hox* genes during MN pool differentiation. These studies indicate that Hox proteins contribute to neuronal fate and muscle connectivity through controlling the levels and pattern of cell surface receptor expression, consequently gating the ability of MNs to respond to limb-derived instructive cues.

## Graphical Abstract

Correspondence: jeremy.dasen@nyumc.org.

**Author Contributions**

C.C., M.M.S. and J.S.D conceived and designed the study. D.H.L provided technical assistance, and J.P.L. generated reagents essential for the studies. C.C. and J.S.D wrote the manuscript.

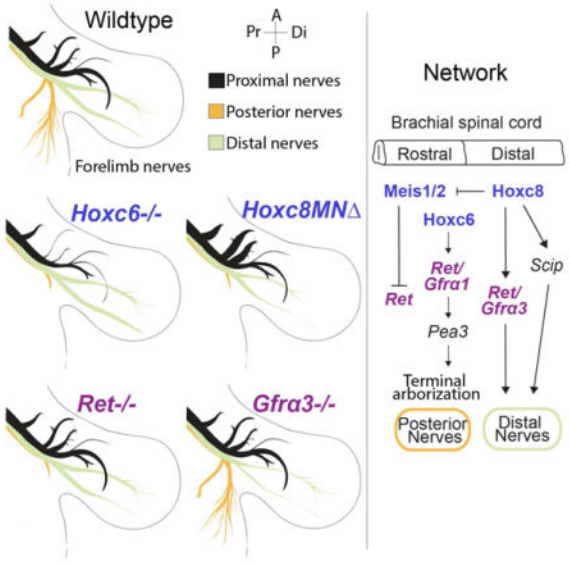


## Introduction

Correct wiring of nervous systems involves both cell intrinsic factors that contribute to neuronal subtype identities and cell surface recognition systems that facilitate the connectivity of individual neurons. Although synaptic specificity determinants have been described in many systems (Dudanova and Klein, 2013; Kolodkin and Tessier-Lavigne, 2011; Sanes and Yamagata, 2009); the regulatory mechanisms governing the expression of guidance and adhesion molecules are poorly defined. Cell fate determinants likely play a key role in orchestrating synaptic specificity programs, but there are few examples where the relationships between transcription networks and cell surface receptors have been established (Polleux et al., 2007; Santiago and Bashaw, 2014; Zarin et al., 2014b).

Progress towards defining how neuronal identity directs connectivity has emerged through analysis of guidance decisions within the vertebrate spinal cord (Bonanomi and Pfaff, 2010; Klein and Kania, 2014). MNs targeting limb muscles are contained within the lateral motor columns (LMCs), which further differentiate into divisional and pool subtypes targeting specific limb regions (Landmesser, 2001). Neurons within the lateral division of the LMC innervate dorsal limb muscles, while medial LMC neurons project ventrally (Landmesser, 1978a; Tosney and Landmesser, 1985). MN pools positioned rostrally within the LMC typically pursue an anterior/proximal trajectory, while those residing more caudally innervate more posterior/distal limb muscles (Hollyday and Jacobson, 1990; Landmesser, 1978b). Experimental manipulations that alter MN or limb bud position indicate that motor axons can redirect their trajectories to find their appropriate targets (Ferguson, 1983; Lance-Jones and Landmesser, 1980, 1981; Stirling and Summerbell, 1988), suggesting that groups of MNs within the LMC are intrinsically programmed to select a specific pathway in response to limb-derived cues.

Depletion of factors involved in LMC subtype differentiation often disrupts the specificity of muscle target innervation, presumably due to changes in the expression of surface

receptors on motor axons. For example, the Lim homeodomain (HD) transcription factors Lhx1 and Isl1 control expression of *Eph* guidance receptors and dictates the initial trajectories of motor axons at the base of the limb. Lhx1 induces expression of *Epha4* in the lateral division of the LMC to direct motor axons dorsally within the limb, while Isl1 promotes *Ephb1* expression in medial LMC neurons to direct axons ventrally (Helmbacher et al., 2000; Kania and Jessell, 2003; Luria et al., 2008). With the exception of this relatively simple binary decision, the mechanisms that restrict expression of surface receptors within specific MN subtypes are poorly understood.

A large family of transcription factors critical for MN subtype differentiation and connectivity are encoded by the *Hox* gene clusters, which comprise 39 genes organized in 4 chromosomal arrays (Philippidou and Dasen, 2013). Studies in chick have shown that *Hox* genes are differentially expressed by MNs along the rostrocaudal axis, and a network of ~20 Hox proteins defines the identities of MN pools targeting specific limb muscles (Dasen et al., 2003; Dasen et al., 2005; Liu et al., 2001). However, whether the pattern of *Hox* gene expression in MNs is predictive of muscle target specificity is largely untested, and the precise requirements for the majority of *Hox* genes are not well established. Moreover, with the exception of a handful of downstream transcription factors, the target effectors of Hox proteins in MNs are yet to be determined.

In this study we assessed the mechanisms through which *Hox* genes control expression of cell surface receptors during MN subtype differentiation. We show that MNs extending along the major nerves within the forelimb are defined by specific profiles of Hox expression, and that *Hox* genes are essential in establishing the pattern and specificity of limb muscle innervation. *Hox* genes determine MN pool fates and connectivity patterns through controlling the profile of *Ret* and *Gfrα* expression, and by constraining the ability of MNs to respond to limb-derived signals. We suggest that *Hox* genes govern neuronal fate and target connectivity by defining both the level and pattern of cell surface receptor gene expression.

## Results

### Hox Profiles Define MN Groups Targeting Forelimb Muscles

To explore the relationship between profiles of Hox protein expression in MNs and peripheral target specificity, we first sought to establish a detailed molecular map of MN groups targeting forelimb and shoulder muscles in mice. We determined the position of MNs projecting along the nine major nerve pathways within the forelimb at embryonic stage (e) 12.5 (Figure 1A–B). Consistent with studies in postnatal rat and embryonic chick (Bacskai et al., 2013; Hollyday and Jacobson, 1990; Tosolini and Morris, 2012), MNs targeting proximal forelimb muscles were located in rostral spinal segments, while MNs projecting distally were positioned caudally. Furthermore, ventrally located MNs adopted a proximal trajectory whereas distal limb muscles were innervated by dorsally located MNs (Figure 1B, S1A–I).

We next determined the profile of Hox protein expression in traced MN populations. We assessed the expression of Hoxc4, Hoxa5, Hoxc5, Hoxc6 and Hoxc8 as well as Hox co-

factors belonging to the Meis and Pbx families. We found that Hox5, Meis1, Meis2, Pbx1 and Pbx3 proteins were restricted to rostral brachial LMC neurons, while Hoxc8 was expressed caudally (Figure 1D, E, G and Figure S1J–L). Neurons within the $Hox5^{+}$ and $Hoxc8^{+}$ populations could be further distinguished by differential expression of additional Hox proteins. While all rostral LMC neurons express Hoxc5, Hoxa5 was excluded from axillary MNs (Figure 1D, E). Hoxc4 was present in a subset of rostral $Hox5^{+}$ LMC neurons (Figure 1C); while Hoxc6 was excluded from MNs targeting specific proximal and distal nerves (Figure 1F). Some MNs projecting along motor nerves shared identical or similar Hox codes, but could be discriminated by differential expression of the Lim HD proteins Lhx1 and Isl1 (Figure S1M,N). These results indicate that the expression of Hox proteins, Hox cofactors, and Lim HD proteins mark subsets of MNs supplying forelimb and shoulder muscles (Figure 1H).

### *Hox* Genes are Essential for MN Topographical Organization and Innervation Pattern

To assess the function of *Hox* genes in the organization and connectivity of MNs we analyzed mice lacking *Hox5 (Hoxa5* and *Hoxc5), Hoxc6*, and *Hoxc8*, as well as the *HoxC* gene cluster. We determined how loss of *Hox* function affects the differentiation of LMC neurons, the overall pattern of limb innervation, and the topographic relationship between MN position and target muscle specificity. Each *Hox* mutant line was crossed with *Hb9::GFP* mice to visualize motor axon projection patterns, and to assist in the identification of nerves for tracing assays.

Analysis of mice lacking *Hox5* genes in MNs ($Hox5^{MN\Delta}$*;Hb9::GFP* mice) (Philippidou et al., 2012) revealed grossly normal patterns of limb innervation (Figure S2A,B), and expression of Hoxc4, Hoxc6, Meis and Foxp1 proteins was preserved (Figure S2I and data not shown). Because assessment of axonal trajectories alone does not provide information on whether MNs make appropriate decisions to target a specific region, we performed retrograde labeling assays in $Hox5^{MN\Delta}$*;Hb9::GFP* mice. Retrograde tracing from the suprascapular nerve labeled MNs that were scattered within the LMC and expressed high levels of Hoxc4 (Figure S2J), a profile typically observed for lateral pectoral MNs. Because the profile of Hoxc4 expression is unchanged in $Hox5^{MN\Delta}$ mice (Figure S2I), these results indicate that some MNs lacking *Hox5* genes adopt aberrant routes and target inappropriate muscles.

*Hoxc8* is expressed by caudal brachial LMC neurons that innervate distal and posterior limb muscles. Within these segments MN pools targeting the cutaneous maximus (CM) and anterior latissimus dorsi (ALD) muscles are defined by expression of the transcription factor Pea3, while median and ulnar MNs express Scip (Jung et al., 2010; Livet et al., 2002). In mice lacking *Hoxc8* in MNs ($Hoxc8^{MN\Delta}$ mice) there was a marked reduction in expression of these markers (Figure S2M,N and O). Consistent with this defect, the median and ulnar nerves were thinner, the median nerve was truncated, and terminal arbors at the CM and ALD muscles were dramatically reduced (Figure 2A,B,E,F, S2A,B,E,F). Retrograde tracing from the ulnar, median, medial anterior thoracic and radial nerves revealed that MNs were scattered within the LMC in *Hoxc8* mutants, in contrast to the stereotypic positioning and clustered organization in controls (Figure 2N–P, S2P).

*Hoxc8* has been shown to be required for the exclusion of *Hox5* genes from caudal LMC neurons in chick (Dasen et al., 2005). In *Hoxc8*$^{MN\Delta}$ mice we observed a caudal extension of multiple rostrally-restricted factors, including Hoxc4, Hoxa5, Meis and Pbx proteins (Figure S2Q,R and data not shown). The diameters of nerves originating from rostral Hox5$^{+}$ LMC neurons were increased in *Hoxc8*$^{MN\Delta}$ embryos (Figure 2I), suggesting that some caudal LMC neurons are redirected to targets of Hox5$^{+}$ MNs. To test this we performed retrograde tracing assays from the suprascapular and lateral pectoral nerves, revealing a caudal extension of Hox5$^{+}$ MN pools (Figure 2J–M). To further assess whether a fate switch occurred in *Hoxc8* mutants, we took advantage of a *LacZ* reporter inserted into the *Hoxc8* locus. Staining for β Galactosidase (βGal) indicated that MNs within the caudal LMC coexpressed Hoxa5, Meis2, and βGal in *Hoxc8* mutants (Figure S2S,T). Furthermore, MNs projecting along the suprascapular and lateral pectoral nerves expressed βGal in *Hoxc8* mutants (Figure S2U,V). These studies suggest that in *Hoxc8* mutants there is a partial transformation of caudal LMC neurons to a Hox5$^{+}$ fate.

*Hoxc6* is required for the expression of *Pea3* and the innervation of the CM and ALD muscles (Figure 2C,D, S2C,D) (Lacombe et al., 2013). Further analysis of *Hoxc6−/−;Hb9::GFP* mice revealed additional defects not present in either *Hox5* or *Hoxc8* mutants. The diameters of the axillary, lateral pectoral and radial nerves were reduced by ~50% in *Hoxc6* mutants while ulnar nerve diameters were increased by 31% (Figure 2C,D,I). Retrograde labeling assays revealed that MNs projecting along the lateral pectoral, radial and median anterior thoracic nerves were disorganized (Figure 2Q–S, S2K,L). Mice lacking the *HoxC* cluster displayed MN phenotypes that were a composite of defects in *Hoxc6* and *Hoxc8* mutants, including altered nerve diameters and a lack of intramuscular arborization at the CM and ALD muscles (Figure 2G,H,I, S2G,H). Collectively these analyses reveal essential roles for *Hox* genes in establishing the appropriate pattern of forelimb innervation and MN pool organization.

## Ret and Gfrα Receptors are Selectively Expressed by Subsets of LMC Neurons

What are the effectors of Hox proteins in MNs, how are they regulated, and how do they contribute to LMC topographic organization and connectivity? To address these questions, we screened for surface receptors whose expression patterns correlated with Hox profiles along the rostrocaudal axis or within a single segment. One group of genes which met these criteria included the receptor tyrosine kinase *Ret* and members of its *Gfrα* coreceptors. Analysis of *Ret* in brachial LMC neurons revealed striking differences in expression levels along the rostrocaudal axis (Figure 3A–B, S3A–B). In rostral Hox5$^{+}$ LMC neurons, MNs expressed low levels of *Ret* mRNA and protein relative to the caudal Hoxc8$^{+}$ domain which expressed high levels at e12.5 (Figure 3A,B,E,F).

Ret signaling is mediated by Gfrα receptors, which upon ligand binding dimerize and activate specific downstream signaling cascades. Selective expression of *Gfrα* genes has been reported in subsets of MNs (Gould and Oppenheim, 2004; Gu and Kania, 2010; Homma et al., 2003), and we therefore assessed the expression pattern of each of the four murine *Gfrα* receptors. *Gfrα1* expression was broadly expressed by brachial MNs at e12.5, with elevated levels observed within the caudal LMC (Figure 3C). *Gfrα3* was restricted to a

caudal subpopulation of LMC neurons that overlapped with the position of Scip$^+$ MNs (Figure 3D, G, S3C). *Gfrα2* was weakly expressed by brachial MNs while *Gfrα4* was not detected (Figure S3D and data not shown).

Comparison of *Ret* and *Gfrα* expression between mouse and chick revealed largely conserved profiles, with a few notable differences (Figure 2O,P, S3F). As in mouse, high levels of *Ret* mRNA and protein were detected in caudal Hoxc8$^+$ LMC neurons in chick, while lower levels were present in rostral Hoxa5$^+$ MNs (Figure 3H,I,L,M). *Gfrα1* displayed a more restricted pattern in chick than in mouse, with high levels of expression overlapping with the position of Pea3$^+$ MNs (Figure 3J,N, S3F). In contrast to mouse, *Gfrα2* expression was present in a lateral population of brachial MNs in chick, while *Gfrα3* was not detected (Figure S3E and data not shown). In chick *Gfrα4* expression was similar to mouse *Gfrα3*, occupying a position overlapping with Scip$^+$ LMC neurons (Figure 3K,N, S3F).

### *Ret* and *Gfrα3* are Downstream Targets of Hox Proteins in LMC Neurons

To determine whether the MN organization and connectivity defects observed in *Hox* mutants are due to loss of Ret/Gfrα signaling components, we analyzed *Hox* mutant mice for changes in *Ret* and *Gfrα* expression. We assessed *Ret* mRNA in *Hoxc6*, *Hoxc8$^{MN\Delta}$* and *HoxC* mutant animals and compared expression with control littermates at e12.5. We also quantified the levels of Ret protein in mutant lines and control littermates. This analysis revealed a pronounced reduction in both *Ret* mRNA and protein levels in the posterior Hoxc8$^+$ region in *Hoxc6*, *Hoxc8*, and *HoxC* cluster mutants (Figure 4A–I). *Ret* expression was present in caudal LMC neurons, but reduced to levels comparable to those observed in rostral Hox5$^+$ neurons.

We also examined the expression of *Gfrα* genes in *Hox* mutants. Expression of *Gfrα3* was markedly decreased in *Hoxc8$^{MN\Delta}$* and *HoxC$^{-/-}$* embryos, but was grossly normal in *Hoxc6* mutants (Figure 4J–O, S4B). Expression of *Gfrα1* was largely unaffected in *Hoxc6*, *Hoxc8$^{MN\Delta}$*, and *HoxC* mutants at e12.5 (Figure S4A,B). These results show that *Hox* genes contribute to the differential expression of *Ret* in LMC neurons along the rostrocaudal axis, and are essential for the intrasegmental pattern of *Gfrα3*.

### *Hox* Network Interactions Determine the Profiles of *Ret*/*Gfrα* Genes in MNs

Our analyses indicate that multiple *Hox* genes are necessary to define *Ret/Gfrα* expression in LMC neurons, but also raise the question of how interactions amongst Hox proteins contribute to their specific patterns. We first determined whether *Hox* genes are sufficient to induce *Ret* and *Gfrα* expression outside their normal domains. We misexpressed *Hox* genes in the neural tubes of stage (st) 13 chick embryos using the *chicken β-actin* (*CAGGs*) promoter, and analyzed *Ret*, *Gfrα1* and *Gfrα4* expression at st27. We found that both *Hoxc6* and *Hoxc8* are sufficient to induce high levels of *Ret* at thoracic levels, where *Ret* levels are normally low (Figure 5A,D,E,H and S5A,C). In contrast misexpression of the rostrally expressed *Hox* genes, *Hoxc4* and *Hoxa5*, did not induce *Ret* at any level (Figure S5I–L).

Both Hoxc6 and Hoxc8 can impose an LMC fate on thoracic MNs through induction of the transcription factor *Foxp1* (Dasen et al., 2008; Lacombe et al., 2013). The elevated levels of

*Ret* observed upon thoracic *Hoxc6* and *Hoxc8* misexpression therefore could be indirect, due to the actions of Foxp1. To determine if Foxp1 can elevate *Ret* expression independent of *Hox* genes, we misexpressed *Foxp1* at rostral cervical and thoracic levels. After misexpression of *Foxp1* elevated *Ret* expression was not observed at either level (Figure S5G,H and data not shown). These results indicate that Foxp1 alone is insufficient to promote the high levels of *Ret* observed in caudal LMC neurons.

Hoxc6 is expressed in rostral Hox5$^+$ LMC neurons, yet is presumably incapable of promoting high *Ret* levels in this region. We tested whether factors present in rostral LMC neurons contribute to the reduced levels of *Ret*. Misexpression of Meis1 in caudal Hoxc8$^+$ LMC neurons, where *Ret* levels are relatively high, resulted in a marked inhibition of *Ret* expression (Figure 5I,L and S5E,F). In contrast, misexpression of *Hoxc4*, *Hoxa5*, *Pbx1* and *Pbx3* did not alter *Ret* expression in caudal LMC neurons (Figure S5M–P and data not shown).

Although Hoxc6 and Hoxc8 were both capable of elevating *Ret* levels, they each promoted distinct patterns of *Gfrα* expression and MN pool identities. Hoxc6, but not Hoxc8, induced expression of *Gfrα1* in cervical MNs, where expression of this receptor is normally low (Figure 5B, S5D). This result is consistent with the observation that in chick *Gfrα1* is restricted to the Hoxc6$^+$, Pea3$^+$ MN pool, but excluded from Scip$^+$ MNs. In addition, Hoxc8 was able to induce expression of *Gfrα4* at thoracic levels (Figure 5F, S5B), while Meis1 repressed both *Gfrα1* and *Gfrα4* at caudal brachial levels (Figure 5J,K). Hoxc6 and Hoxc8 also promoted distinct MN pool fates, with Hoxc6 inducing Pea3 expression and Hoxc8 inducing Scip at thoracic levels (Figure 5C,G) (Lacombe et al., 2013).

These results indicate that regulatory interactions amongst Hoxc6, Hoxc8, and Meis1 define the patterns of *Ret*, *Gfrα1* and *Gfrα4* in brachial LMC neurons (Figure 5Y). Hoxc6 and Hoxc8 are sufficient to induce elevated *Ret* levels, while Meis1 dampens *Ret* expression in rostral LMC neurons. Hoxc6 promotes expression of *Gfrα1* within MN pools defined by Pea3 expression, while Hoxc8 promotes *Gfrα4* and a Scip$^+$ MN pool identity.

## Hox and Meis Regulatory Interactions Control *Ret* Expression in Lumbar LMC Neurons

Our analyses of *Ret* gene regulation at brachial levels are seemingly at odds with studies in lumbar LMC neurons, where *Ret* is essential during dorsoventral projection decisions (Kramer et al., 2006). Dorsally-projecting lateral LMC (LMCl) neurons express high levels of *Ret* while medial LMCm neurons express low levels. In the absence of *Ret*, LMCl motor axons fail to pursue a dorsal trajectory along the peroneal nerve (Bonanomi et al., 2012; Kramer et al., 2006). To determine whether *Ret* expression in lumbar LMC neurons is defined by similar Hox-regulatory interactions, we assessed whether *Hox* genes expressed at lumbar levels can induce *Ret* expression. We found that after misexpression of the lumbar LMC determinants *Hoxc10* and *Hoxd10* elevated levels of *Ret* were detected in thoracic MNs (Figure 5S–V).

Because Meis1 is involved in dampening *Ret* expression in rostral brachial MNs, we asked whether it is also involved in restricting *Ret* to lumbar LMCl neurons. In both mouse and chick Meis1 expression was restricted to the LMCm at lumbar levels and only weakly

detected in LMCl neurons (Figure 5M–R). Moreover, misexpression of *Meis1* at lumbar levels repressed *Ret* expression in LMCl neurons (Figure 5W,X). These observations indicate that the pattern of *Ret* expression in brachial and lumbar LMC neurons is defined by a common Hox/Meis regulatory strategy (Figure 5Y,Z).

### Ret and Gfrα1 Activities Bypass the Requirement for *Hox* Genes in *Pea3* Induction

What is the functional significance of the profile of *Ret* and *Gfrα* genes during MN differentiation? The ligand for Ret/Gfrα1 receptors, Gdnf, is broadly expressed in the periphery (Haase et al., 2002; Jung et al., 2010), suggesting that MN responsiveness to peripheral signals is constrained by LMC-intrinsic factors. To test this we asked whether elevating *Ret* and *Gfrα1* outside their normal domains affects MN pool differentiation. We expressed *Ret* and *Gfrα1* by *in ovo* electroporation at rostral brachial and thoracic levels, where expression of these genes is normally low, and assessed expression of *Pea3*, a known target of Gdnf-Ret/Gfrα1 signaling (Haase et al., 2002). Elevating *Ret* expression at thoracic levels, but not in rostral LMC neurons, generated ectopic Pea3$^{+}$ MNs (Figure 6A–D, S6E). The selective induction of Pea3 at thoracic levels appears to stem from the fact that thoracic MNs in chick also express *Gfrα1* (Figure S6A), creating a condition where MNs now express both *Ret* and *Gfrα1*. Consistent with this idea; upon coexpression of *Ret* and *Gfrα1* in either rostral brachial or thoracic MNs we observed induction of *Pea3* expression (Figure 6I–N, Q). In contrast, expression of *Gfrα1* in either rostral LMC or thoracic segments was insufficient to induce *Pea3* (Figure 6E–H).

Induction of *Pea3* after misexpression of *Ret* and *Gfrα1* did not lead to ectopic expression of LMC-associated transcription factors such as Hoxc6, Hoxc8, or Foxp1 (Figure S6B–D). These observations indicate that *Pea3* induction can occur independently of an earlier LMC specification program, implying that a key function of *Hox* genes is to establish the domain in which the Pea3$^{+}$ MN pool can be specified. High levels of *Ret* in combination with *Gfrα1* expression appears therefore to define the competence of MNs to express *Pea3* (Figure 6R). Given that in *Pea3* mutants there is a selective loss in terminal branches at the CM muscle (Livet et al., 2002), these results suggest the CM innervation defects observed in *Hoxc8* and *Hoxc6* mutants are due to the loss of *Pea3* induction by Ret/Gfrα1 signaling.

### *Ret* and *Gfrα3* Mutants Display Innervation Defects Similar to *Hox* Mutants

To assess whether attenuation of Ret/Gfrα signaling contributes to the MN defects observed in *Hox* mutants, we analyzed mice lacking *Ret* and *Gfra3*. Previous analysis of *Ret* mutants revealed essential roles in the innervation of dorsal hindlimb muscles (Bonanomi et al., 2012; Kramer et al., 2006), and *Gdnf* and *Gfrα1* mutants have been shown to be required for the induction of *Pea3* at brachial levels (Haase et al., 2002). However the role of *Ret* in the specification and connectivity of LMC neurons has not been fully established. In *Ret* mutants expression of Hoxc6, Hoxc8, and Foxp1 was preserved at e12.5 and e13.5, consistent with a function downstream of *Hox* genes (Figure S7A–C and data not shown). However, there was a marked reduction in the number of MNs expressing *Pea3* (Figure 7A, B). Interestingly, the total number of Scip$^{+}$ MNs was increased by 38% in *Ret*$^{-/-}$ embryos, leading to a ventral expansion of this pool (Figure 7C, D). Conversely, generating ectopic Pea3 neurons, via misexpression of *Ret* and *Gfrα1*, led to a marked reduction in the number

of Scip$^{+}$ neurons (Figure 6O–Q). These results indicate that the establishment of the normal distribution of Pea3$^{+}$ and Scip$^{+}$ MNs relies on *Ret* function.

We next analyzed the pattern of limb innervation in *Ret* mutants. Similar to *Hoxc6*$^{-/-}$, *Hoxc8*$^{MN\Delta}$, and *Pea3*$^{-/-}$ mice (Livet et al., 2002), *Ret*$^{-/-}$ embryos displayed a marked loss in axonal arbors at the CM and ALD muscles (Figure 7E–H). Projections along the ulnar and median nerves were present in *Ret*$^{-/-}$*:Hb9::GFP* mice, but displayed aberrant branches along the ulnar nerve, resulting in thinning of this nerve distally (Figure 7G,H,N). Retrograde tracing of MNs projecting along the median and ulnar nerves labeled MNs positioned more ventrally, as observed in *Hoxc8* mutants (Figure 7J,K). In contrast, tracing from the medial anterior thoracic nerve in *Ret* mutants labeled MNs positioned more dorsally, similar to *Hoxc6* and *Hoxc8* mutants (Figure 7I).

We next analyzed mice lacking *Gfrα3*, which is restricted to Scip$^{+}$ MNs. In *Gfrα3;Hb9::GFP* mice both the median and ulnar nerves were thinner at e13.5 (Figure 7L–N), similar to *Hoxc8*$^{MN\Delta}$ mice. However, in contrast to *Hoxc8*$^{MN\Delta}$ and *Ret* mutant mice, retrograde labeling from the median and ulnar nerves in *Gfrα3* mutants indicated a grossly normal organization (Figure S7D, E). Given that in *Hoxc8* mutants median and ulnar MNs are disorganized, these results indicate that *Gfrα3* mutation does not phenocopy loss of *Hoxc8*, and that Hox proteins have additional targets required for motor pool clustering. The number of Scip$^{+}$; Foxp1$^{+}$ MNs was unchanged in *Gfrα3* mutants (Figure S7F), suggesting that the innervation defects are due to an inability of motor axons to fully extend within the limb. Collectively these results indicate that *Ret* and *Gfrα3* mutants display limb innervation defects similar to *Hox* mutants.

## Discussion

Networks of transcription factors are critical for neuronal subtype diversification, but how cell fate determinants orchestrate expression of surface receptors is poorly understood. In this study we found that *Hox* genes are essential for the organization and peripheral connectivity of MNs targeting the forelimb, and identified *Ret* and *Gfrα* genes as key targets of their actions. We discuss these findings in the context of transcriptional and signaling networks conferring MN-muscle target specificity, and consider the possible mechanisms contributing to the diversification of limb innervation programs in tetrapods.

### *Hox* Genes Govern MN Diversity and Peripheral Innervation Pattern

*Hox* genes are essential for neuronal specification in the hindbrain and spinal cord (Philippidou and Dasen, 2013; Tumpel et al., 2009), but the extent to which they define the connectivity of limb-innervating MNs is unclear. LMC neurons segregate into ~50 MN pools, each pool defined by its connectivity to a single limb muscle. While certain MN pools express subtype-restricted factors, whether a selective transcriptional code defines each subtype is unknown. We found that MNs extending along the nine major forelimb nerve pathways are defined by restricted patterns of Hox proteins and Hox cofactors. *Hox5* genes define MNs that target proximal/anterior limb regions, *Hoxc8* distal/posterior regions, with additional *Hox* genes and cofactors contributing to MN diversity and connectivity within these broad domains. In principle, additional layers of target specificity could be imparted

by differences in Hox protein levels between MN pools, which may grade surface receptor expression. In support of this idea, level-dependent activities of Hox proteins in MNs have been demonstrated during the innervation of leg muscles in *Drosophila* (Baek et al., 2013).

Consistent with roles in establishing the identity and connectivity of LMC neurons, removal of *Hox* genes leads to defects in the pattern of limb innervation, and dissolves the normal topographic relationship between MN position and target specificity. Mutation of individual *Hox* genes causes a deterioration of MN organization and peripheral target specificity along multiple nerves. However, with the exception of the CM and ALD muscles, most targets appear to receive at least some innervation in the absence of *Hox* genes. These observations are in agreement with analysis of *Foxp1* mutants, where Hox-dependent LMC programs are lost, and MNs target limb muscles in a stochastic manner (Dasen et al., 2008; Rousso et al., 2008). Therefore in the absence of *Hox* genes motor axons can continue to pursue trajectories along the available paths within the limb, but appear to lose the ability to select appropriate targets.

The most severe deficits after removal of *Hox* genes are apparent upon assessment of the relationship between MN position and target specificity. *Hox* mutants display specific defects in the normal topographic organization and position of MN pools. In *Hoxc8* mutants MNs targeting the distal forelimb are disorganized within the LMC, and a subset of MNs lacking *Hoxc8* target proximal forelimb muscles normally supplied by $Hox5^+$ populations. These observations suggest that in *Hoxc8* mutants there is a partial transformation of LMC neurons to a $Hox5^+$ fate and connectivity pattern. Although it is unclear whether similar fate transformations occur in each of the *Hox* mutants we analyzed, their phenotypes likely reflect loss of guidance systems that dictate the selection of one peripheral innervation pathway over another.

## Hox Target Effectors in Neuronal Fate Specification and Axon Guidance

The ability of motor axons to navigate towards and innervate peripheral targets with precision relies upon the selective expression of cell surface receptors. Combinatorial sets of transcription factors are known to be essential for neuronal subtype diversification, but how intrinsic factors shape MN identities and innervation pattern is poorly defined. Studies in *Drosophila* have shown that the transcription factor Hb9 acts in ventrally projecting MNs to regulate expression of the *Robo2* guidance receptor, while in dorsally projecting MNs, Eve2 controls expression of the *Unc5* gene (Santiago et al., 2014; Zarin et al., 2014a). In vertebrates, motor axon guidance in the limb bud is known to require the activities of a variety of genes, including *Ret*, *Epha4*, *Ephb1*, *Frizzled3*, *Npn1*, and *Celsr3* (Bonanomi and Pfaff, 2010; Hua et al., 2013; Santiago and Bashaw, 2014). However, beyond the contribution of Lim HD proteins to the selection of dorsal and ventral limb trajectories, how fate determinants orchestrate MN connectivity is poorly understood.

We found that Hox/Hox cofactor interactions define the spatial profiles of *Ret* and *Gfrα* genes in MNs, and signaling through Ret/Gfrα receptors is essential in Hox-dependent programs of MN differentiation and connectivity. During MN pool specification, activation of Ret/Gfrα1 signaling by Gdnf is required for *Pea3* expression in a subset of LMC neurons (Haase et al., 2002). Application of Gdnf throughout the spinal cord however induces *Pea3*

only within the caudal LMC populations that would have expressed it normally. This suggests the existence of intrinsic systems that limit MN responses to Gdnf. Our results indicate that Hox/Meis interactions define the pattern of *Ret* and *Gfra1* in caudal LMC neurons, thereby restricting the ability of peripheral cues to induce *Pea3* expression. In support of this idea, elevating *Ret* and *Gfrα1* throughout the spinal cord is sufficient to activate *Pea3*, bypassing the requirement for *Hox* genes. *Hox* genes therefore appear to constrain MN responsiveness to peripheral cues by selectively regulating expression of surface receptors.

In addition to contributing to MN pool diversification, signaling through Ret is essential during motor axon guidance decisions. In the hindlimb, *Ret* is required for the selection of a dorsal trajectory by LMC axons, acting in part by modulating signaling through Eph receptors (Bonanomi et al., 2012). We found that Hox/Meis regulatory interactions determine the spatial profiles of *Ret* expression in LMC neurons, and silencing *Ret* and *Gfrα3* causes innervation defects similar to those observed after selective removal of *Hox* genes. In the absence of *Ret*, projections towards posterior and distal muscle groups are deteriorated, similar to the innervation defects observed in *Hoxc6* and *Hoxc8* mutants. These phenotypes appear to be due in part to the loss of *Pea3*, as *Pea3* mutants display a severe reduction in intramuscular branches at the CM muscle (Livet et al., 2002). Our studies show that loss of *Ret* and *Gfrα3* also leads to innervation defects in the distal forelimb, raising the possibility that Ret/Gfrα signaling contributes to guidance decisions independent of *Pea3* regulation.

### *Hox* Genes and the Evolution of Limb Innervation Programs

The musculoskeletal system of the forelimb varies significantly amongst vertebrates, raising the question of how MN specification programs evolved to accommodate different motor behaviors. The basic topographical organization of MNs is conserved amongst all tetrapods that have been examined (Fetcho, 1992), and evolutionary modification of *Hox* activities appears to have contributed to changes in LMC position relative to the limbs (Jung et al., 2014). During the evolution of paired-appendages, the appearance of new muscle groups enabled species to achieve greater complexity in the range of limb movements. This process presumably required an expansion of MN subtype identites from a more simplified ancestral population. The Lim HD code governing dorsoventral projections appears to be present in pectoral fins of zebrafish (Uemura et al., 2005), suggesting this program appeared prior to land invasion. As the number of muscle groups expanded in early vertebrates, *Hox5* and *Hox8* paralogs could have been coopted to govern the innervation of proximal/anterior and distal/posterior muscles respectively. Subsequently the actions of *Hox4*, *Hox6*, and *Hox7* genes further diversified MN pools to allow for more selective targeting of limb muscles.

Comparison of limb innervation programs in mice and chick suggests the existence of diversification programs acting downstream of *Hox* genes. Both birds and rodents appear to share a common Hox/Ret/Gfrα-based regulatory strategy for specifying $Pea3^{+}$ MN pools. However, there are significant functional differences between the muscle groups targeted by these neurons. In birds $Pea3^{+}$ MNs target the pectoralis (Pec), a large muscle providing the major driving force for flexing the wing during flight (Biewener, 2011; Hollyday and

Jacobson, 1990). By contrast, in mice most Pea3$^+$ MNs target the cutaneous maximus, a subcutaneous muscle present in fur-bearing mammals, with no known role in locomotion. We found that in chick *Gfrα1* is restricted to the Pea3$^+$ pool, while in mice *Gfrα1* is broadly expressed by LMC neurons. Differences in the regulation of *Gfrα* genes by Hox proteins may have contributed to the evolutionary divergence of muscle-specific connectivity programs in birds in mammals.

In summary these studies indicate that *Ret* and *Gfrα* genes are key targets of Hox proteins during MN specification and the establishment of limb innervation pattern. Given that one feature of Hox activity is to define *Ret* levels in MNs, it is plausible that additional target effectors are under similar graded control mechanisms. Regulation of the levels of receptor gene expression could represent a common regulatory strategy through which networks of transcription factors establish neuronal subtype identities and determine target specificity.

## Experimental Procedures

### Animals

All mouse procedures were approved by the Institutional Animal Care and Use Committee of the New York University School of Medicine.

### *In situ* Hybridization and Immunohistochemistry

Embryos were harvested between e11.5–14.5 and fixed in 4% paraformaldehyde for 1.5–2 hours and processed for *in situ* hybridization or immunohistochemistry. For wholemount immunohistochemistry, embryos were processed for GFP staining as previously described (De Marco Garcia and Jessell, 2008). Confocal images were obtained with a Zeiss (LSM 700) microscope and analyzed with ImageJ software.

### Retrograde Labeling of MNs

Embryos were harvested at e12.5, eviscerated and forelimb nerves were visualized using a MVX10 wide-field fluorescent microscope (Olympus). The nerve of interest was cut and injected with lysine fixable Rhodamine-dextran (Molecular Probes). Embryos were incubated for 3.5–4.5 hours in oxygenated DMEM/F12 (50:50) solution at 30–34°C, fixed, and processed for immunohistochemistry.

### *In ovo* Chick Embryo Electroporations

Electroporations were performed at Hamburger and Hamilton (HH) st12–14 chick embryos as previously described (Dasen et al., 2003). Plasmid concentrations ranged from 100–500 ng/μl and pBKS was used as carrier DNA to achieve a final concentration of 1 μg/μl. Results for each experiment are representative of five or more embryos in which the electroporation efficiency in MNs was >50%.

### Quantifications and Statistical Analyses

Cell counting was performed using ImageJ software in at least three embryos per genotype. Cells stained for Foxp1, Pea3, or Scip were counted and aligned by comparison of LMC position between littermates. Nerve thickness was analyzed by measuring the length of a

line running perpendicular to the long axis of the nerve. For consistent comparison, measurements were taken in similar regions of the nerves between littermates. Ret fluorescence intensities were measured using ImageJ software as described previously (Gavet and Pines, 2010), with some modifications. For fluorescence measurements, we used the following formula for each section of at least three animals per genotype: $Foxp1^+$ cells signal = sum of the intensity of pixels for $Foxp1^+$ cells. Background signal = average signal per pixel for a region selected just beside $Foxp1^+$ cells. $Foxp1^+$ Ret fluorescence signal = $Foxp1^+$ cell signal – surface selected (number of pixels for the selected area) x background. Statistical significance was determined with the unpaired two-tailed Student's t-test using Microsoft Excel. *P < 0.05; **P < 0.01; ***P < 0.001.

## Supplementary Material

Refer to Web version on PubMed Central for supplementary material.

## Acknowledgments

We thank Myungin Baek, Gord Fishell, Heekyung Jung, and Polyxeni Philippidou for comments on the manuscript, and Rocio Rivera for preliminary analyses of *Hoxc8* mutants. This work was supported by funding from the NIH (R01 NS062822), and an NIH predoctoral training grant (T32NS086750) to M.M.S.

## References

Bacskai T, Fu Y, Sengul G, Rusznak Z, Paxinos G, Watson C. Musculotopic organization of the motor neurons supplying forelimb and shoulder girdle muscles in the mouse. Brain Struct Funct. 2013; 218:221–238. [PubMed: 22362202]

Baek M, Enriquez J, Mann RS. Dual role for Hox genes and Hox co-factors in conferring leg motoneuron survival and identity in Drosophila. Development. 2013; 140:2027–2038. [PubMed: 23536569]

Biewener AA. Muscle function in avian flight: achieving power and control. Philos Trans R Soc Lond B Biol Sci. 2011; 366:1496–1506. [PubMed: 21502121]

Bonanomi D, Chivatakarn O, Bai G, Abdesselem H, Lettieri K, Marquardt T, Pierchala BA, Pfaff SL. Ret is a multifunctional coreceptor that integrates diffusible- and contact-axon guidance signals. Cell. 2012; 148:568–582. [PubMed: 22304922]

Bonanomi D, Pfaff SL. Motor axon pathfinding. Cold Spring Harb Perspect Biol. 2010; 2:a001735. [PubMed: 20300210]

Dasen JS, De Camilli A, Wang B, Tucker PW, Jessell TM. Hox repertoires for motor neuron diversity and connectivity gated by a single accessory factor, FoxP1. Cell. 2008; 134:304–316. [PubMed: 18662545]

Dasen JS, Liu JP, Jessell TM. Motor neuron columnar fate imposed by sequential phases of Hox-c activity. Nature. 2003; 425:926–933. [PubMed: 14586461]

Dasen JS, Tice BC, Brenner-Morton S, Jessell TM. A Hox regulatory network establishes motor neuron pool identity and target-muscle connectivity. Cell. 2005; 123:477–491. [PubMed: 16269338]

De Marco Garcia NV, Jessell TM. Early motor neuron pool identity and muscle nerve trajectory defined by postmitotic restrictions in Nkx6.1 activity. Neuron. 2008; 57:217–231. [PubMed: 18215620]

Dudanova I, Klein R. Integration of guidance cues: parallel signaling and crosstalk. Trends Neurosci. 2013; 36:295–304. [PubMed: 23485451]

Ferguson BA. Development of motor innervation of the chick following dorsal-ventral limb bud rotations. J Neurosci. 1983; 3:1760–1772. [PubMed: 6886745]

Fetcho JR. The spinal motor system in early vertebrates and some of its evolutionary changes. Brain Behav Evol. 1992; 40:82–97. [PubMed: 1422809]

Gavet O, Pines J. Progressive activation of CyclinB1-Cdk1 coordinates entry to mitosis. Dev Cell. 2010; 18:533–543. [PubMed: 20412769]

Gould TW, Oppenheim RW. The function of neurotrophic factor receptors expressed by the developing adductor motor pool in vivo. J Neurosci. 2004; 24:4668–4682. [PubMed: 15140938]

Gu WX, Kania A. Examining the combinatorial model of motor neuron survival by expression profiling of trophic factors and their receptors in the embryonic Gallus gallus. Dev Dyn. 2010; 239:965–979. [PubMed: 20108351]

Haase G, Dessaud E, Garces A, de Bovis B, Birling M, Filippi P, Schmalbruch H, Arber S, deLapeyriere O. GDNF acts through PEA3 to regulate cell body positioning and muscle innervation of specific motor neuron pools. Neuron. 2002; 35:893–905. [PubMed: 12372284]

Helmbacher F, Schneider-Maunoury S, Topilko P, Tiret L, Charnay P. Targeting of the EphA4 tyrosine kinase receptor affects dorsal/ventral pathfinding of limb motor axons. Development. 2000; 127:3313–3324. [PubMed: 10887087]

Hollyday M, Jacobson RD. Location of motor pools innervating chick wing. J Comp Neurol. 1990; 302:575–588. [PubMed: 1702118]

Homma S, Yaginuma H, Vinsant S, Seino M, Kawata M, Gould T, Shimada T, Kobayashi N, Oppenheim RW. Differential expression of the GDNF family receptors RET and GFRalpha1, 2, and 4 in subsets of motoneurons: a relationship between motoneuron birthdate and receptor expression. J Comp Neurol. 2003; 456:245–259. [PubMed: 12528189]

Hua ZL, Smallwood PM, Nathans J. Frizzled3 controls axonal development in distinct populations of cranial and spinal motor neurons. Elife. 2013; 2:e01482. [PubMed: 24347548]

Jung H, Lacombe J, Mazzoni EO, Liem KF Jr, Grinstein J, Mahony S, Mukhopadhyay D, Gifford DK, Young RA, Anderson KV, et al. Global control of motor neuron topography mediated by the repressive actions of a single hox gene. Neuron. 2010; 67:781–796. [PubMed: 20826310]

Jung H, Mazzoni EO, Soshnikova N, Hanley O, Venkatesh B, Duboule D, Dasen JS. Evolving Hox activity profiles govern diversity in locomotor systems. Dev Cell. 2014; 29:171–187. [PubMed: 24746670]

Kania A, Jessell TM. Topographic motor projections in the limb imposed by LIM homeodomain protein regulation of ephrin-A:EphA interactions. Neuron. 2003; 38:581–596. [PubMed: 12765610]

Klein R, Kania A. Ephrin signalling in the developing nervous system. Curr Opin Neurobiol. 2014; 27:16–24. [PubMed: 24608162]

Kolodkin AL, Tessier-Lavigne M. Mechanisms and molecules of neuronal wiring: a primer. Cold Spring Harb Perspect Biol. 2011; 3

Kramer ER, Knott L, Su F, Dessaud E, Krull CE, Helmbacher F, Klein R. Cooperation between GDNF/Ret and ephrinA/EphA4 signals for motor-axon pathway selection in the limb. Neuron. 2006; 50:35–47. [PubMed: 16600854]

Lacombe J, Hanley O, Jung H, Philippidou P, Surmeli G, Grinstein J, Dasen JS. Genetic and functional modularity of Hox activities in the specification of limb-innervating motor neurons. PLoS Genet. 2013; 9:e1003184. [PubMed: 23359544]

Lance-Jones C, Landmesser L. Motoneurone projection patterns in the chick hind limb following early partial reversals of the spinal cord. J Physiol. 1980; 302:581–602. [PubMed: 7411470]

Lance-Jones C, Landmesser L. Pathway selection by embryonic chick motoneurons in an experimentally altered environment. Proc R Soc Lond B Biol Sci. 1981; 214:19–52. [PubMed: 6121329]

Landmesser L. The development of motor projection patterns in the chick hind limb. J Physiol. 1978a; 284:391–414. [PubMed: 731552]

Landmesser L. The distribution of motoneurones supplying chick hind limb muscles. J Physiol. 1978b; 284:371–389. [PubMed: 731549]

Landmesser LT. The acquisition of motoneuron subtype identity and motor circuit formation. Int J Dev Neurosci. 2001; 19:175–182. [PubMed: 11255031]

Liu JP, Laufer E, Jessell TM. Assigning the positional identity of spinal motor neurons: rostrocaudal patterning of Hox-c expression by FGFs, Gdf11, and retinoids. Neuron. 2001; 32:997–1012. [PubMed: 11754833]

Livet J, Sigrist M, Stroebel S, De Paola V, Price SR, Henderson CE, Jessell TM, Arber S. ETS gene Pea3 controls the central position and terminal arborization of specific motor neuron pools. Neuron. 2002; 35:877–892. [PubMed: 12372283]

Luria V, Krawchuk D, Jessell TM, Laufer E, Kania A. Specification of motor axon trajectory by ephrin-B:EphB signaling: symmetrical control of axonal patterning in the developing limb. Neuron. 2008; 60:1039–1053. [PubMed: 19109910]

Philippidou P, Dasen JS. Hox genes: choreographers in neural development, architects of circuit organization. Neuron. 2013; 80:12–34. [PubMed: 24094100]

Philippidou P, Walsh CM, Aubin J, Jeannotte L, Dasen JS. Sustained Hox5 gene activity is required for respiratory motor neuron development. Nat Neurosci. 2012; 15:1636–1644. [PubMed: 23103965]

Polleux F, Ince-Dunn G, Ghosh A. Transcriptional regulation of vertebrate axon guidance and synapse formation. Nat Rev Neurosci. 2007; 8:331–340. [PubMed: 17453014]

Rousso DL, Gaber ZB, Wellik D, Morrisey EE, Novitch BG. Coordinated actions of the forkhead protein Foxp1 and Hox proteins in the columnar organization of spinal motor neurons. Neuron. 2008; 59:226–240. [PubMed: 18667151]

Sanes JR, Yamagata M. Many paths to synaptic specificity. Annu Rev Cell Dev Biol. 2009; 25:161–195. [PubMed: 19575668]

Santiago C, Bashaw GJ. Transcription factors and effectors that regulate neuronal morphology. Development. 2014; 141:4667–4680. [PubMed: 25468936]

Santiago C, Labrador JP, Bashaw GJ. The homeodomain transcription factor Hb9 controls axon guidance in Drosophila through the regulation of Robo receptors. Cell Rep. 2014; 7:153–165. [PubMed: 24685136]

Stirling RV, Summerbell D. Specific guidance of motor axons to duplicated muscles in the developing amniote limb. Development. 1988; 103:97–110. [PubMed: 3197635]

Tosney KW, Landmesser LT. Development of the major pathways for neurite outgrowth in the chick hindlimb. Dev Biol. 1985; 109:193–214. [PubMed: 2985457]

Tosolini AP, Morris R. Spatial characterization of the motor neuron columns supplying the rat forelimb. Neuroscience. 2012; 200:19–30. [PubMed: 22100785]

Tumpel S, Wiedemann LM, Krumlauf R. Hox genes and segmentation of the vertebrate hindbrain. Curr Top Dev Biol. 2009; 88:103–137. [PubMed: 19651303]

Uemura O, Okada Y, Ando H, Guedj M, Higashijima S, Shimazaki T, Chino N, Okano H, Okamoto H. Comparative functional genomics revealed conservation and diversification of three enhancers of the isl1 gene for motor and sensory neuron-specific expression. Dev Biol. 2005; 278:587–606. [PubMed: 15680372]

Zarin AA, Asadzadeh J, Hokamp K, McCartney D, Yang L, Bashaw GJ, Labrador JP. A transcription factor network coordinates attraction, repulsion, and adhesion combinatorially to control motor axon pathway selection. Neuron. 2014a; 81:1297–1311. [PubMed: 24560702]

Zarin AA, Asadzadeh J, Labrador JP. Transcriptional regulation of guidance at the midline and in motor circuits. Cell Mol Life Sci. 2014b; 71:419–432. [PubMed: 23917723]

## Highlights

A Hox code defines MNs projecting along the major axes of the limb

*Ret* and *Gfrα* genes are key targets of Hox proteins in limb-innervating MNs

Hox/Hox cofactor interactions govern *Ret* levels and *Gfrα* patterns in MNs

Loss of *Ret* and *Gfrα3* causes MN defects similar to *Hox* gene mutations

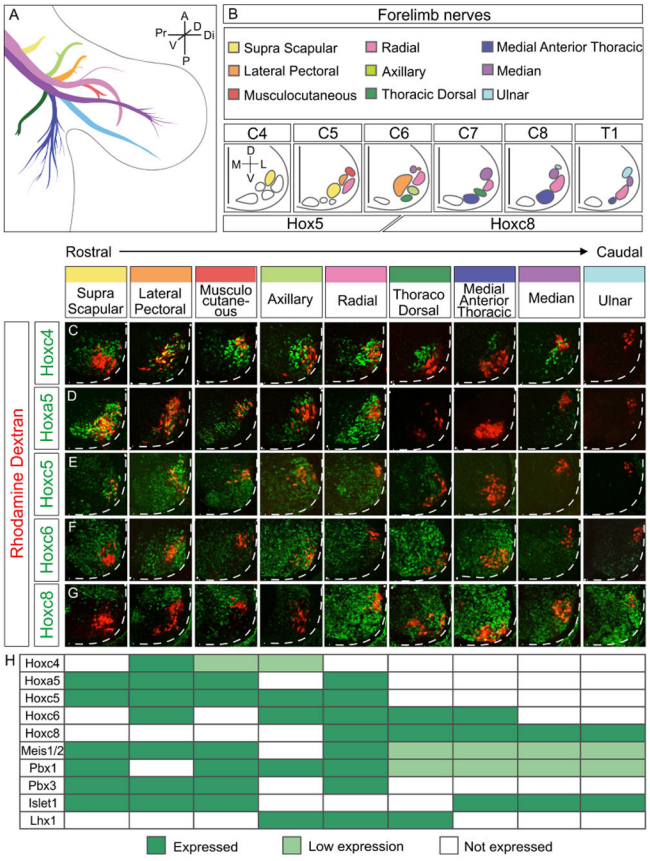


**Figure 1. Combinatorial Hox Profiles Define Forelimb Innervating MNs**

(A) Schematic of the primary motor nerves supplying the mouse forelimb at e12.5. Dorso-ventral (D–V), medio-lateral (M–L) and proximo-distal (Pr-Di) axes are indicated. (B) Topographical organization of forelimb MNs. MN positions are based on retrograde labeling from nerves at e12.5 (see Figure S1A–I). Dorso-ventral (D–V) and medio-lateral (M–L) coordinates are indicated. Segmental position of labeled LMC neurons are indicated, and extend from cervical segment 4 (C4) to thoracic segment 1 (T1). Non-LMC MN populations present in these segments are also outlined. (C–G) Hoxc4, Hoxa5, Hoxc5, Hoxc6 and Hoxc8 expression in retrogradely labeled MNs projecting along the suprascapular, lateral pectoral, musculocutaneous, axillary, thoracodorsal, medial anterior lateral, radial, median and ulnar nerves. (H) Summary of Hox expression profiles in MNs projecting along the main forelimb motor nerves. See also Figure S1.

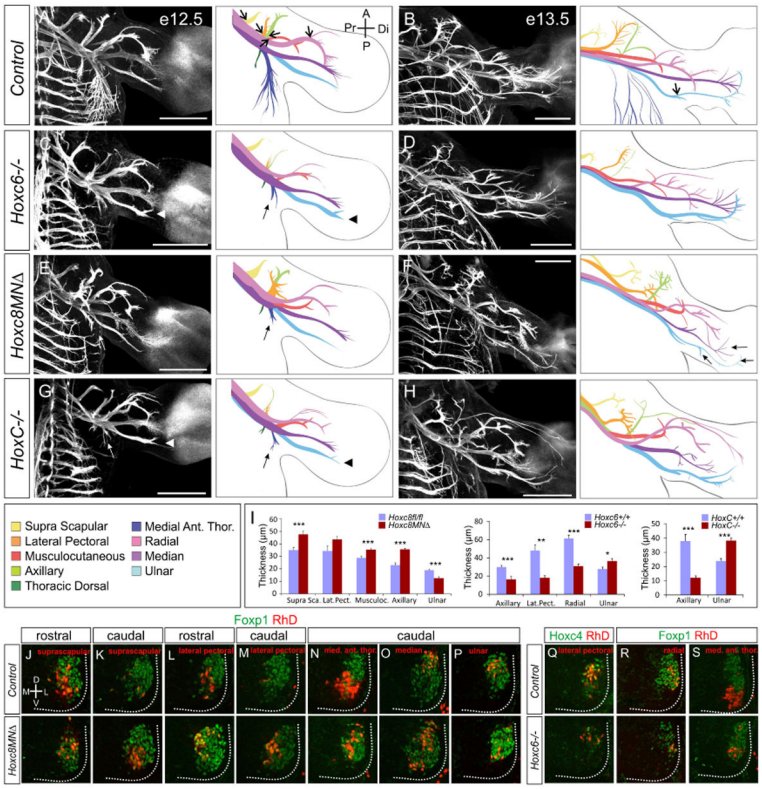


**Figure 2. *Hox* Genes Govern Limb Innervation Pattern and MN Pool Organization**

(A–B) Wholemount GFP staining of control *Hb9::GFP* mice at e12.5 and e13.5. Schematic representations of innervation pattern are shown in right panels and motor nerves are color coded. Arrows indicate region where nerve diameters were measured. (C–H) Forelimb innervation patterns in *Hoxc6*, *Hoxc8* and *HoxC* mutants at e12.5 and e13.5. Arrows and arrowheads indicate major nerve defects. Scale-bars represent 500 μm. Innervation patterns in control littermates are shown in Figure S2. (I) Quantification of muscle nerve diameters in indicated *Hox* mutant lines. Data are shown as mean +/− S.E.M. (J–P) Retrograde labeling of MNs in *Hoxc8* mutants. *Hoxc8* mutants display defects in the organization of suprascapular, lateral pectoral, medial anterior thoracic, median and ulnar MNs. (Q–S) Retrograde labeling of MNs projecting along the lateral pectoral, medial anterior thoracic and radial nerves in *Hoxc6* mutants. The position and organization of MNs projecting along the suprascapular and musculocutaneous nerves are not affected in *Hoxc6* mutants (Figure S2K, L). See also Figure S2.

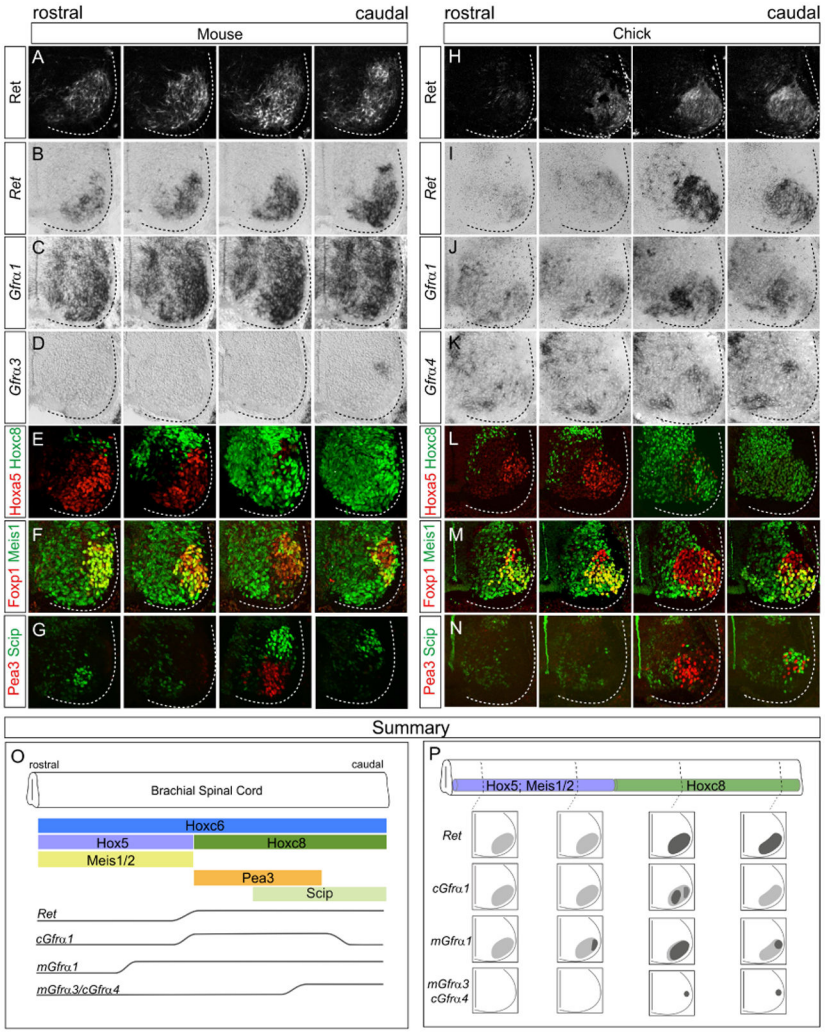


**Figure 3. Expression of *Ret* and *Gfrα* Genes in LMC Neurons**

(A–G) Expression patterns of *Ret*, *Gfrα1* and *Gfrα3* in MNs along the rostrocaudal axis, aligned with expression of Hoxa5, Hoxc8, Meis1/2, Foxp1, Pea3 and Scip at e12.5. (H–N) Expression of Ret, *Gfrα1* and *Gfrα4* in MNs aligned with Hoxa5, Hoxc8, Meis1/2, Foxp1, Pea3 and Scip in chick at st29. (O) Summary of the expression profiles of mouse (m) and chick (c) *Ret*, *mGfrα1*, *cGfrα1*, *mGfrα3* and *cGfrα4* along the rostrocaudal axis. Expression domains of Hoxa5, Hoxc8, Meis1/2, Hoxc6, Pea3 and Scip are depicted for positional comparison. (P) Summary of the intrasegmental expression profile of *Ret*, *mGfrα1*, *cGfrα1*, *mGfrα3* and *cGfrα4* in brachial MNs. See also Figure S3.

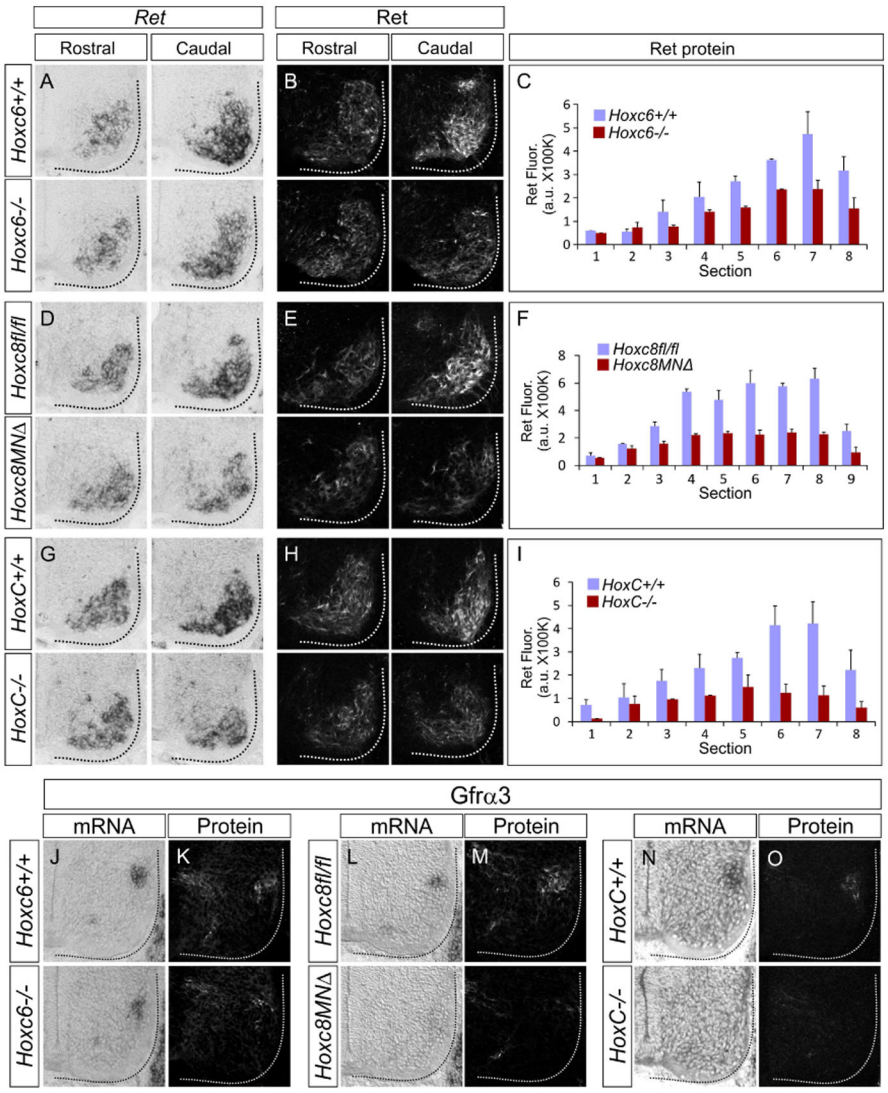


**Figure 4. Multiple *Hox* Genes Establish *Ret* and *Gfrα* Profiles in LMC neurons**

(A–H) Analysis of *Ret* expression in *Hox* mutant mice at e12.5. *Ret* levels are attenuated in *Hoxc6*, *Hoxc8* and *HoxC* mutants within caudal LMC neurons. *Ret* mRNA and protein levels are shown in the indicated mutants and control littermates. Panels C, F and I show quantification of Ret antibody immunofluorescence from serial sections along the rostrocaudal axis (see Experimental Procedures). Data are shown as mean +/− S.E.M. (J–O) *Gfrα3* expression is markedly downregulated in *Hoxc8* and *HoxC* mutants but preserved in *Hoxc6* mutants. See also Figure S4.

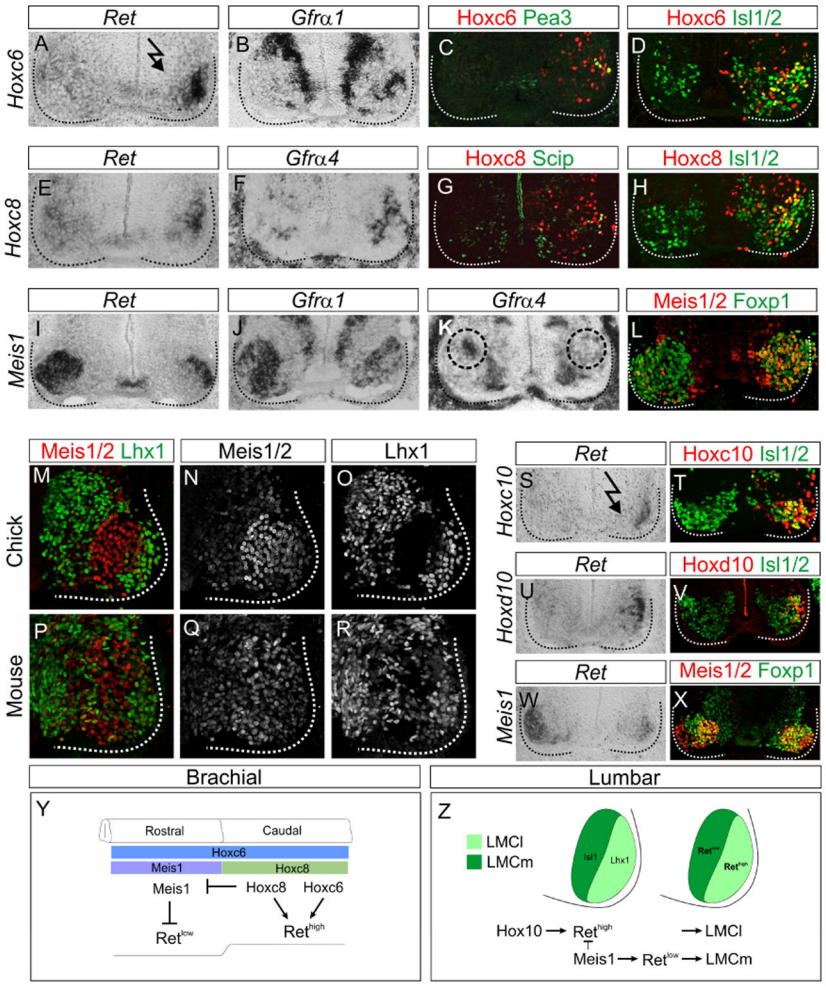


**Figure 5. Hox and Meis Interactions Govern Ret Expression in LMC Neurons**

(A–D) Electroporation of *Hoxc6-pCAGGs* induces *Ret* and *Pea3* expression at thoracic levels and *Gfrα1* at rostral cervical levels. Hoxc6 and Isl1/2 costaining is shown to indicate electroporated MNs. Arrow in panel A indicates electroporated side of embryo. (E–H) Electroporation of *Hoxc8-pCAGGs* induces *Ret*, *Gfrα4* and *Scip* expression at thoracic levels. (I–L) Misexpression of *Meis1* represses *Ret*, *Gfrα1* and *Gfrα4* in caudal LMC neurons. (M–R) Expression of Meis1/2 and Lhx1 in chick and mouse lumbar LMC neurons. In both chick and mouse Meis1/2 expression is reduced in lateral Lhx1$^{+}$ MNs, which express high levels of Ret. (S–V) Electroporation of *Hoxc10* and *Hoxd10* induces expression of *Ret* at thoracic levels. (W,X) *Meis1* misexpression represses *Ret* in lumbar LMC neurons. (Y) Summary of *Ret* regulation by Hox/Hox co-factors in brachial LMC neurons. (Z) Summary showing regulation of *Ret* by Hox/Hox co-factors at lumbar levels. See also Figure S5.

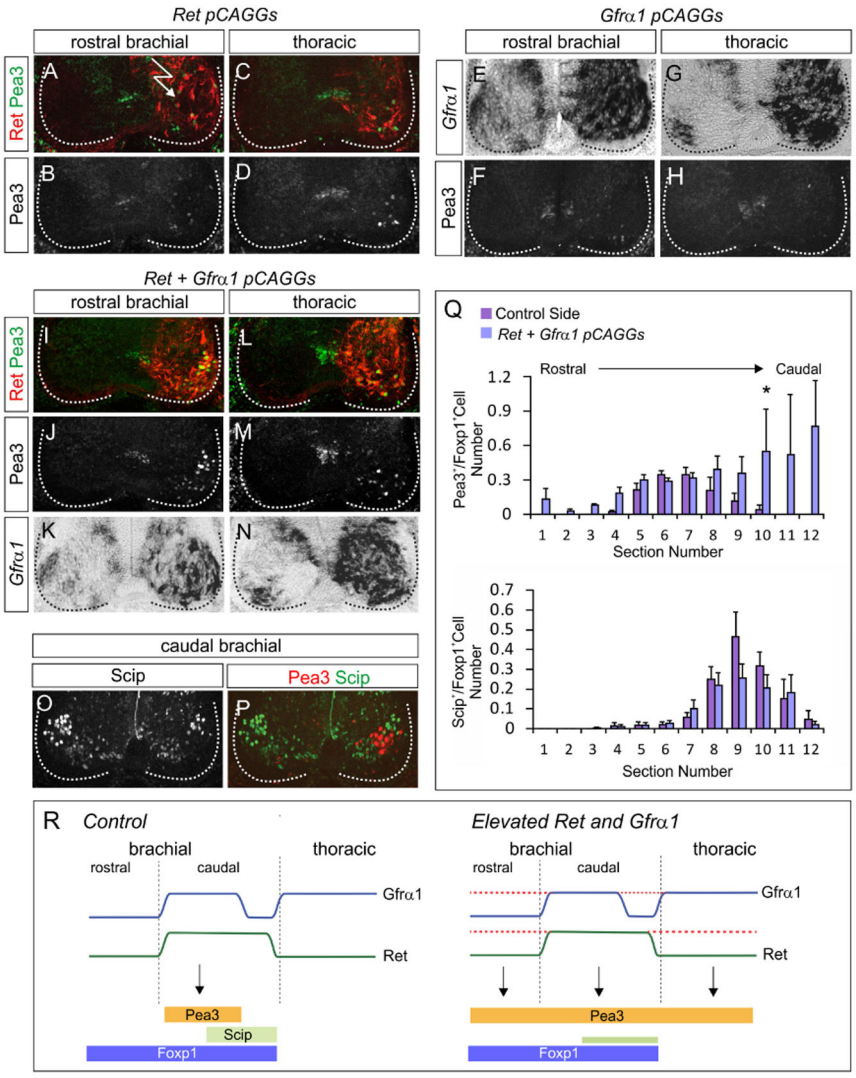


**Figure 6. *Ret* and *Gfrα1* Patterns Facilitate *Pea3* Induction in MN Pools**

(A–D) Misexpression of *Ret* under *pCAGGs* induces *Pea3* expression in thoracic MNs but not rostral brachial LMC neuron. (E–H) *Gfrα1* missexpression fails to induce *Pea3* expression in rostral brachial and thoracic MNs. (I–N) Co-expression of *Ret* and *Gfrα1* is sufficient to induce Pea3 at both rostral brachial and thoracic levels. (O–P) After induction of *Pea3* by *Ret* and *Gfrα1* there is a reduction in the number of $Scip^+$ LMC neurons. (Q) Quantification showing increased numbers of $Pea3^+$ and reduced $Scip^+$ MNs along the rostrocaudal axis after *Ret* and *Gfrα1* misexpression. Numbers are representative of electroporation experiments with efficiencies of greater than 50%. (R) Diagram summarizing the relationship between *Ret*, *Gfrα1*, *Scip* and *Pea3* expression, as well as the effects of *Ret* and *Gfrα1* misexpression on the differentiation of $Pea3^+$ and $Scip^+$ MN pools. See also Figure S6.

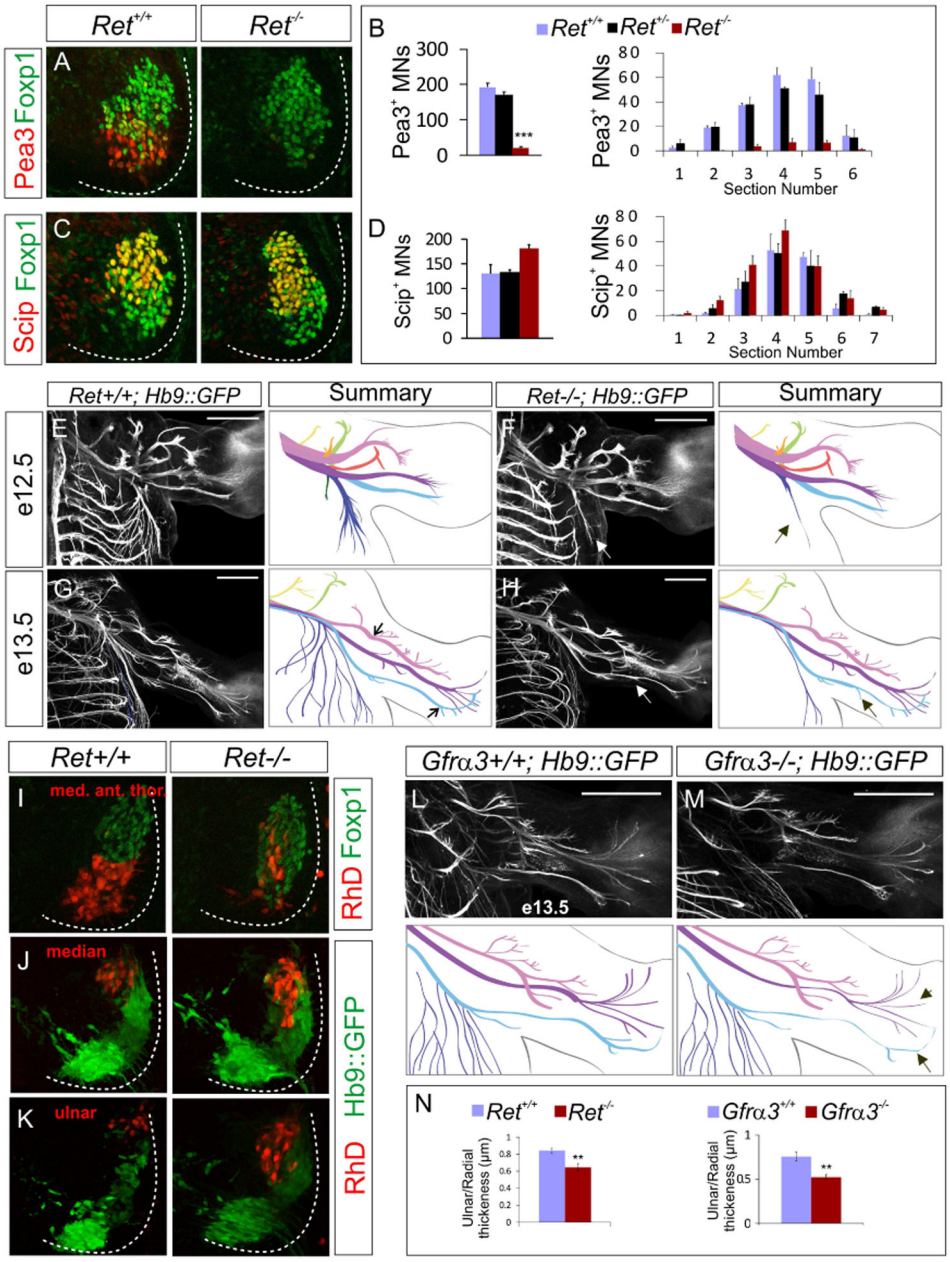


**Figure 7. *Ret* and *Gfrα3* are Required for MN Pool Differentiation and Connectivity**

(A) Pea3 expression is reduced in brachial LMC neurons in *Ret* mutants at e12.5. (B) Quantification of the number and distribution of Pea3$^+$ MNs in *Ret*−/− and control mice. (C) The number of Scip$^+$ MNs increases in *Ret*−/− mice. (D) Quantification of the number and distribution of Scip$^+$ MNs. (E,F) Wholemount GFP staining showing defects in CM muscle innervation in *Ret*−/− embryos (arrow) at e12.5. (G,H) Forelimb innervation at e13.5 showing failure of ulnar MNs to project distally in *Ret*−/− embryos (arrow). Arrows in control diagram indicate region where nerve diameters were measured. (I–K) Disorganization of MNs in *Ret*−/− mice shown by retrograde labeling of MNs projecting along the medial anterior thoracic, median and ulnar nerves. (L,M) Forelimb innervation

pattern in *Gfrα3*+/+ and *Gfrα3*−/− mice at e13.5 showing thinning of the median and ulnar nerves. Scale-bars represent 500 μm. (N) Quantification of muscle nerve diameters expressed as a ratio between the radial and ulnar nerves in *Ret* and *Gfrα3* mutants and controls at e13.5. See also Figure S7.